CLM-P335





CLM-P335


UKAEA RESEARCH GROUP

Preprint

# AN EXPERIMENTAL VERIFICATION OF PARAMETRIC RESONANCE INSTABILITY THEORY

S AIHARA
V A DIXON
J JANCARIK
G LAMPIS
S TAKAMURA
C J H WATSON

CULHAM LABORATORY
Abingdon Berkshire

1972

CLM-P 335

# AN EXPERIMENTAL VERIFICATION OF PARAMETRIC RESONANCE INSTABILITY THEORY

by

S. Aihara*, V.A. Dixon+, J. Jancarik**, G. Lampis≠, S. Takamura∅ and C.J.H. Watson

(Submitted for publication in Plasma Physics)

ABSTRACT

The theory of the parametric resonance instability due to Silin predicts a shift in the frequency of ion acoustic waves propagating in a plasma in the presence of a high frequency electric field. An experiment has been performed in which ion acoustic waves spontaneously produced in a back-diffusion type plasma exhibit an increase in their frequency, when a radiofrequency electric field is applied. The validity of the theory of Silin is confirmed by the experiment.

* Institute of Plasma Physics, Nagoya University, Nagoya, Japan

+ Mathematical Institute, Oxford University, England

** Department of Plasma Physics, University of Texas, Austin, U.S.A.

≠ Association Euratom-CEA, Département de la Physique du Plasma et de la Fusion Contrôlée, Centre d'Etudes Nucléaires, 92 Fontenay-aux-Roses, France

∅ Department of Electronics, Faculty of Engineering, Nagoya University, Nagoya, Japan

UKAEA Research Group,
Culham Laboratory,
Abingdon,
Berks.

November 1972

## 1. INTRODUCTION

The behaviour of plasma in a strong electromagnetic field is of interest for a number of reasons. Such fields can, in principle, be used to confine or accelerate the plasma by exerting radiation pressure on it (Motz, H. and Watson, C.J.H. (1967); Gorbunov, L.M. (1969)), they can be used to stabilise the plasma dynamically (Fainberg, Ya.-B and Shapiro, V.D., (1967); Kornilov, E.A. et al.(1966); Krivoruchko, S.M. and Kornilov, E.A. (1969)), and they can be used to heat it (e.g. by microwave or laser heating.)

In each of these applications a large amplitude coherent electromagnetic wave is created within the plasma : in the first two applications, however, one seeks to establish a stable wave, i.e. one attempts to ensure that no other waves are generated. In the third application one seeks to establish conditions for instability so that a turbulent wave spectrum is set up. The theory of the parametric resonance instability, which is probably the most significant in all of these applications, was given by Silin and his co-workers, (Aliev, Yu.M, and Silin, V.P., (1965); Silin, V.P. (1965); Aliev Yu.M, Silin, V.P., Watson, C.J.H. (1966); Silin, V.P. (1966); Andreev, N.E. et al. (1969); Silin, V.P. (1969)), and this theory has been invoked by Gekker, I.R., Sizukhin, O.V. (1969), Sergheichev, K.F. (1969) and Batanov, G.M. et al. (1969) to explain the rather limited success of current experiments on RF plasma acceleration, and by Kaw, P.K. and Dawson, J.M. (1969) as a possible mechanism for the rapid plasma heating in strong laser focus experiments. The theoretical analysis of Silin is in two parts - in the first part (Silin, V.P. (1965))

he provides an analysis which is wholly non-linear with respect to the amplitude $E_o(\omega_o, k_o)$ of the coherent externally applied electric field of frequency $\omega_o$ and wavenumber $k_o$, but linear with respect to the amplitude $\phi_o(\omega, k)$ of the electrostatic wave spectrum resulting from it. In the second part (Silin, V.P. (1969)) he uses quasi-linear theory to determine the saturation level of this spectrum.

In the present paper we report an experiment which provides satisfactory confirmation of the first part of Silin's analysis, under conditions in which the driving field $E_o$ is sufficiently weak for the saturation level to be relatively low. As a result of the low saturation level and the finite geometry of the experiment, the turbulent frequency spectrum of the waves generated by the instability has a band structure with the amplitude within each band fairly well peaked at one of the discrete set of normal modes of the system. Although many such bands are observed in the experiment, the work reported here relates to the two lowest ion modes, which had wavelengths comparable with the dimensions of the apparatus.

## 2. EXPERIMENTAL APPARATUS AND DIAGNOSTICS

The experimental apparatus is shown in Fig. 1. The vessel in which the plasma is contained is a metallic cylinder having a diameter of 50 cm and a length of 100 cm No magnetic field is applied to the plasma. The plasma is produced by a funnel type plasma source (Takayama, K., Ikegami, H. and Aihara, S. (1967); Takamura, S. et al. (1969)). Helium gas flows from the back side of a hollow

anode A through a leak valve and enters the vessel passing across the four indirectly heated oxided cathodes; the vessel is continuously evacuated and the pressure of the helium gas inside is constant.

The discharge occurs in the funnel shaped tube between the anode A ($V_A \sim +450$ volt) and the cathodes K ($V_K = 0$ volt); the pressure in the narrow glass pipe between A and $G_2$ is of the order of $10^{-1}$ torr; the positively biased grid $G_2$ controls the discharge and prevents the production of low frequency noise in the discharge itself. The plasma streams from the source into the metal vessel, where no plasma is actually produced; the pressure in the vessel is about 1% of that inside the narrow glass pipe.

The ions produced in the discharge are accelerated by the positive potential drops between the grids $G_1$, $G_2$ and the grounded cathodes K; typical values of the voltage of $G_1$ are from + 30 volt to + 280 volt; the voltage of $G_2$ is kept at a higher value than that of $G_1$, from + 40 volt to + 300 volt. The ions accelerated inside the metal vessel are spatially neutralised by the thermal electrons emitted by the hot oxide cathodes.

The gridded probe moveable axially ($\phi$ = 3 cm ) shown in fig. 1 is used for measuring the axial variation of the ion saturation current; the same probe is used for measuring the electron temperature and detects the ion acoustic waves which propagate through the plasma from the region in front of the source where they are produced. The axial probe can be substituted by a multigrid ion energy analyser which faces the ion source and measures the ion energy distribution

in the axial direction. The energy resolution of the analyser is about 1 volt.

The plane probe moveable in the radial direction ($\phi$ = 1.5 cm) is used for calibrating the values of the ion saturation current measured by the axial probe and for measuring the radial variation of the electron density; during the RF measurements it is withdrawn near the wall of the vessel. A radiofrequency electric potential (from 1 MHz up to 20 MHz) is applied between a transverse plane rectangular electrode (whose dimensions are 5 cm × 8 cm) and the electrically grounded metal vessel; a second electrode of equal shape and area, opposite to the first, and kept electrically floating, is used for collecting the RF current transmitted across the plasma. Both RF electrodes are kept sufficiently far from the plasma source so that the plasma parameters ($n_e$ and $T_e$) are not changed during the RF injection; moreover, since the ion acoustic waves propagate in the axial direction and since, for maximum coupling, it is desirable to have the direction of the RF field as far as possible parallel to the direction of propagation, an optimum situation is found by setting the planar RF electrodes at 45° to the axis of the vessel. The normal distance between the electrodes is kept at the optimum value of 12 cm. The amplitude of the RF voltage applied to the transmitting electrode is monitored by a vacuum tube voltmeter; the RF current received by the opposite electrode is fed to a 50 Ω load; the output voltage is measured by a second vacuum tube voltmeter.

The ion acoustic waves, produced by a two-stream

instability in front of the exhaust of the source, are collected by the axial moveable receiving probe, biased negatively to reject electrons, and are studied by means of a spectrum analyser (Tektronix mod. IL 5 or Stoddard mod. NM 22A). The frequency spectrum of the ion acoustic waves is displayed on an XY recorder or on an oscilloscope.

## 3. EXPERIMENTAL RESULTS

These measurements represent an extension of previous work on the RF suppression of the amplitude of the spontaneous ion acoustic waves at the sheath plasma resonance (Lampis, G. et al. (1968)) and on the study of the wavelength shift of externally excited ion acoustic waves in the presence of an RF electric field (Takamura, S. et al. (1970); Aihara, S. et al. (1971); Takamura, S. et al. (1971)). The measurements reported here relate to the radiofrequency-induced frequency shift of the spontaneous ion acoustic waves produced in the back diffusion type plasma; such an effect was first reported by Aihara, S., Takamura, S. and Lampis, G. (1970).

The temperature of the plasma electrons, measured by the Langmuir probe method is $T_e \simeq 1$ eV and is the same throughout the vessel. The electron density near the outlet of the source, measured by the same technique, is between $10^7$ cm$^{-3}$ and $10^8$ cm$^{-3}$ depending on the discharge conditions; the density decreases exponentially with the axial distance measured from the cathodes; the e-folding distance is 13 cm (fig. 2). From the Langmuir probe measurements, the electrons in the plasma are found to be purely thermal, with no electron beam present.

The energy distribution of the ions accelerated by the source is doubly peaked; the lower energy peak corresponds to the voltage of the grid $G_1$ located behind the cathode, while

the higher energy peak corresponds to the voltage of the grid $G_2$ near the neck of the source; the lower energy peak has smaller amplitude than the higher energy one.

The ions produced in the funnel between $G_2$ and $G_1$, where the gas pressure drops, are accelerated by the local potential which is equal to or lower than $V_{G_2}$ and constitute the higher energy beam. Since $G_1$, being near to the hot cathodes, is surrounded by an electron sheath, where the electric potential drops, potential troughs are formed between its wires, thus allowing the passage of the beam and its broadening toward energies even lower than $V_{G_1}$. The lower energy beam at $V_{G_1}$ is formed by the ions produced in the secondary discharge between $G_1$ and the cathodes.

The plasma can be considered as a combination of the thermal electrons provided by the cathodes and of two parallel ion beams having different velocities which are slower than the thermal velocity of the electrons by about a factor 5.

Fig. 3 shows a typical measured ion energy distribution taken for $V_{G_1}$ = + 70 volt, $V_{G_2}$ = + 90 volt at a distance of 6 cm from the cathodes; the datum of Fig. 3 was taken during a run different from those related to the subsequent radiofrequency measurements. The precise shape of the ion distribution function varies significantly from run to run. However the width of each beam was observed to be typically in the region 5 - 10 eV, which is well within the energy resolution of the analyser (about 1 volt). Such widths, observed in the laboratory frame, correspond to rather small widths ($\sim$ 0.1 eV) in the frame of the beam, and these are fully consistent with the beam temperatures selected in the theoretical interpretation below. When the radiofrequency measurements were performed the

ion energy distribution was not measured and, as a consequence, the relative amplitudes of the two peaks of the distribution were not known experimentally; however, during all the measurements, as mentioned above, the two peaks in the ion energy distribution correspond exactly to the voltages $V_{G_1}$ and $V_{G_2}$ of the two grids. The total angular divergence of the ion beam, measured by shifting radially a second energy analyser facing the source, varies between $6^{\circ}$ and $9^{\circ}$ according to the conditions of the source itself (higher spread for higher acceleration voltages). An ion acoustic oscillation is spontaneously produced in the plasma by the streaming of the two ion beams through the thermal electrons, the oscillation being strongest at a pressure in the vessel of $1.5 \times 10^{-3}$ torr. (Kawai, Y. et al. (1969)). Higher order modes of oscillation are also observed (Aihara, S. et al. (1968)), but in this paper only the behaviour of the fundamental one is investigated.

The spectrum of the fundamental frequency of the acoustic wave appears as one or sometimes two distinct peaks separated by about 25 kHz. The observed frequency spectrum has the same pattern throughout the plasma volume. Fig. 4 shows a spectrum of the frequency of the fundamental ion acoustic wave; a double peak structure is evident. Spectrum analysis performed in the electron plasma frequency region does not reveal any spontaneous high frequency instability.

The RF voltage, $V_{RF}$, measured on the transmitting electrode, is kept $\leqslant$ 10 volt (rms); the electron temperature, monitored by the Langmuir probe technique during the RF injection, is constant; for values of $V_{RF}$ larger than 10 volt (rms), the intensity of the electric field is so

high that the parameters of the plasma ($n_e$ and $T_e$) begin to change; such a condition is avoided.

During the RF measurements, the electron plasma frequency near the cathodes is $\left(\frac{\omega_{pe}}{2\pi}\right)_a$ = 55 MHz; between the RF electrodes this has fallen to $\left(\frac{\omega_{pe}}{2\pi}\right)_b$ = 11.3 MHz due to the axial and radial density decay. When the RF voltage is kept constant on the transmitting electrode and the frequency is varied, the behaviour of the RF current received by the opposite RF electrode is a typical resonance probe characteristic (Takayama, K., et al. (1960); Harp, R.S. and Crawford, F.W. (1964)) (Fig. 5); the RF current is minimum at the local electron plasma frequency $\frac{\omega_{pe}}{2\pi}$ = 11.3 MHz (in good agreement with the Langmuir probe measurement), and has a maximum at the sheath-plasma frequency $\frac{\omega_R}{2\pi}$ = 5 MHz. Since $\omega_R = \omega_{pe}\left(\frac{S}{L}\right)^{\frac{1}{2}}$, where S/2 is the ion sheath thickness in cm on each electrode and L = 12 cm is the distance between the RF electrodes, we find a value for the sheath thickness $\frac{S}{2}$ = 1.17 cm. Since at the sheath plasma resonance not only the transmitted RF current, but also the RF electric field within the plasma is maximum, the condition of sheath resonance is very useful for achieving a strong interaction between the RF field and the plasma.

The frequency spectrum, explored in the vicinity of the applied RF frequency, shows the appearance of two satellite bands separated from the RF itself by an amount equal to the frequency of the acoustic wave. The amplitude of the two satellite bands is about 2% of that of the injected RF wave; the upper satellite always has a smaller amplitude

than the lower one. The appearance of the satellites is, as we shall see, consistent with the parametric instability theory of Silin described below: however the present paper is concerned with the ion modes themselves rather than these satellites.

The new important observation, whose analysis is the main object of this paper, is the fact that, during the RF injection, the frequency of the spontaneous ion acoustic wave increases with the applied RF voltage and then saturates. Fig. 6, associated to fig. 4, shows the raw data (second experimental run) when, for a constant RF frequency $\frac{\omega_o}{2\pi}$ = 5 MHz, the RF voltage is progressively increased. The double peak structure of the acoustic spectrum is evident as well as the shift of the frequencies of both peaks towards higher values, up to saturation, for increasing RF voltages. For very high RF voltages > 10 volt (rms), the acoustic spectrum flattens (Fig. 6f).

Figs. 7 and 8 present the data taken in the first experimental run, where $V_{G_1}$ was 270 volt and $V_{G_2}$ was 310 volt. For a constant applied RF voltage of 5.5 volt (rms) the frequencies of the upper and lower peaks of the ion acoustic wave vary with the frequency of the applied RF field; the unperturbed upper acoustic wave frequency during this run is 541 kHz; the lower is between 510 and 517 kHz. The maximum increase is found in conditions of sheath-plasma resonance, for the RF field between the electrodes, at $\frac{\omega_o}{2\pi}$ = 5 MHz; this fact confirms that the quantity responsible for changing the ion acoustic wave frequency is the RF electric field, which is maximum at sheath-plasma resonance. It should

perhaps be emphasised that in this experiment, this effect is more important than the achievement of exact parametric resonance conditions. The RF induced frequency shift of the ion acoustic wave is found to increase with increasing values of the unperturbed acoustic frequency. In this work we present data related to acoustic waves whose initial frequency is about 545 kHz, for the upper peak, and about 515 kHz, for the lower peak.

Figure 9 shows, for the data of the first run, how the upper ion wave frequency increases with the applied RF voltage; (in this case the unperturbed ion wave frequency had slightly drifted to 545 kHz with respect to the value of 541 kHz as in the datum of fig. 7). The applied RF field has a fixed frequency of 5 MHz corresponding to the sheath-plasma resonance condition between the RF electrodes. The frequency shift increases with the RF voltage up to $V_{RF}$ = 6 volt (rms) and saturates at $\omega_2 - \omega_{2o}$ = 17 kHz; the maximum fractional frequency shift $\frac{\omega_2 - \omega_{2o}}{\omega_{2o}}$ is 3%.

Figures 10 and 11, corresponding to the second experimental run (the raw data are presented in figures 4 and 6), where the ion acceleration voltages were $V_{G_1}$ = 250 volt and $V_{G_2}$ = 295 volt, show the variation of the frequencies of the upper and lower peaks respectively, versus the applied RF voltage. The RF injection at $\frac{\omega_o}{2\pi}$ = 5 MHz corresponds to the sheath-plasma resonance condition. The maximum fractional frequency shift $\frac{\omega_1 - \omega_{1o}}{\omega_{1o}}$ is larger by about 1% than that of the upper mode.

From the data presented in figures 9, 10 and 11 it

appears that saturation of the frequency shift occurs at $V_{RF}$ = 6 volt (rms), corresponding to a value of the RF electric field in the plasma, calculated in the streaming direction, of about 200 volt $m^{-1}$ (zero to peak value).

The following table gives the values of various physical quantities related to the two interpreted experimental runs:

TABLE

Physical quantities related to the two interpreted experimental radiofrequency injection runs

(Helium gas; $p = 1.4 \times 10^{-3}$ torr.)

$\left(\frac{\omega_{pe}}{2\pi}\right)_a$ = 55 MHz: Electron plasma frequency near the cathodes of the source

$\left(\frac{\omega_{pe}}{2\pi}\right)_b$ = 11.3 MHz: Electron plasma frequency between the RF electrodes

$T_e \simeq 1$ eV : Electron temperature

$\left(\lambda_{De}\right)_a \simeq 0.12$ cm = Debye length near cathodes

$\left(\lambda_{De}\right)_b \simeq 0.6$ cm = Debye length between the RF electrodes

$\frac{\nu_{en}}{2\pi}$ = 1.25 MHz : Electron neutral collision frequency

$\frac{S}{2}$ = 1.17 cm : ion sheath thickness at RF electrodes

L = 12 cm : distance between RF electrodes

First run (Data of figures 7, 8 and 9).

$V_1 = 270$ volt
$V_2 = 310$ volt
} ion acceleration voltages

$v_1 = 1.13 \times 10^5$ m/sec
$v_2 = 1.21 \times 10^5$ m/sec
} velocities of ion beams

$\frac{\omega_{2o}}{2\pi} = 545$ kHz : unperturbed upper ion wave frequency during scanning in $V_{RF}$.

$\frac{\omega_{2o}}{2\pi} = 541$ kHz : unperturbed upper ion wave frequency during scanning in $\omega_o$.

$\frac{\omega_{1o}}{2\pi} = (510 \simeq 517)$ KHz : unperturbed lower ion wave frequency during scanning in $\omega_o$.

Second run (Data of figures 4, 6, 10 and 11).

$V_1 = 250$ volts
$V_2 = 295$ volts
} ion acceleration voltages

$v_1 = 1.09 \times 10^5$ m/sec
$v_2 = 1.18 \times 10^5$ m/sec
} velocities of ion beams

$\frac{\omega_{2o}}{2\pi} = (542 \simeq 545)$ kHz : unperturbed upper ion wave frequency during scanning in $V_{RF}$.

$\frac{\omega_{1o}}{2\pi} = (515 \simeq 521)$ kHz : unperturbed lower ion wave frequency during scanning in $V_{RF}$.

## 4. THEORETICAL INTERPRETATION

The general theory of electrostatic oscillations of an unmagnetized collisionless plasma in an electromagnetic field of peak amplitude $E_o$, frequency $\omega_o$ and wavenumber $k_o$ (assumed much smaller than k, the wavenumber of the electrostatic oscillation) is given by Silin, V.P. (1965).

The equilibrium plasma configuration is defined by the ion and electron distribution functions $f_i \equiv f_i(\vec{v} - \vec{v}_{Ei})$ and $f_e \equiv f_e(\vec{v} - \vec{v}_{Ee})$ where $f_i(u)$ and $f_e(u)$ are arbitrary functions which determine the distribution function which the ions and electrons would possess in the absence of the electromagnetic field, and $v_{Ei}$ and $v_{Ee}$ are the instantaneous velocities of the ions and electrons in a uniform oscillating electric field, given by

$$\vec{v}_{E\alpha} = - \frac{e_\alpha}{m_\alpha \omega_o} \vec{E}_o \cos \omega_o t ,$$

assuming that $\vec{E} = \vec{E}_o \sin \omega_o t$ .

In the present experiment, as we have seen, the electrons are Maxwellian, i.e.

$$f_e(u) \sim e^{-\left(\frac{u}{v_e}\right)^2}$$

and the measured electron temperature (~ 1 eV) gives an electron thermal velocity $v_e = 5.9 \times 10^5$ m/sec. The ion distribution function was not determined experimentally with sufficient precision for it to be regarded as entirely known, although as we have seen it can be represented as a superposition of two ion beams, each having a certain thermal spread which depended on the precise state of the source.

The energies of the two ion beams are (with considerable precision) given by the potentials of the two grids (270 eV,

310 eV in the first run; 250 eV, 295 eV in the second run), but the relative amplitude and the shape of the distribution about these peaks is not known. Accordingly we have taken

$$f_i(u) \sim \beta\, e^{-(u - v_1)^2/v_{i1}^2} + (1 - \beta) e^{-(u - v_2)^2/v_{i2}^2} \qquad (1)$$

where $v_{i1}$ and $v_{i2}$ are the ion thermal velocities of the slower and faster ion beams and $\beta$ is the ratio of the density of the slower ion beam with respect to the total ion density. We have regarded $\beta$, $v_{i1}$ and $v_{i2}$ as free parameters; we shall see that the frequency shift observations permit these parameters to be determined rather accurately, and the values obtained are consistent with typical ion distributions in this experiment.

Following Silin one linearises the Vlasov equation about the (time dependent) equilibrium distribution functions and obtains equations for the perturbed distribution functions $\delta f_e$, $\delta f_i$ and the electrostatic potential $\phi(k,t)$. These quantities can be expanded

$$\phi(k,t) = \sum_{n=-\infty}^{\infty} \phi_n(k,\omega)\, e^{i(\omega + n\,\omega_o)t} \qquad (2)$$

and one obtains a dispersion relation for $\omega$, the (constant) shift away from $n\,\omega_o$ of each harmonic as a function of k (the perturbed wave number), in the form of an infinite determinant. For $\omega \ll \omega_{pe}$ (a condition which is well satisfied in this experiment), in good approximation the dispersion relation reduces to Silin's equation (4.8) (Silin, V.P. (1965)) :

$$1 + \frac{1}{\delta\, \varepsilon_i(\omega, k)} = \sum_{\ell=-\infty}^{\infty} J_\ell^2(a) \left[ \frac{\delta\, \varepsilon_e(\omega + \ell\, \omega_o,\ k)}{1 + \delta\, \varepsilon_e(\omega + \ell\, \omega_o,\ k)} \right] \qquad (3)$$

where $\delta \varepsilon_\alpha(\omega, k) = \frac{\omega_{p\alpha}^2}{k^2} \int \frac{\vec{k} \cdot \frac{\partial f_\alpha(\vec{v})}{\partial v}}{\omega - \vec{k} \cdot \vec{v}} d^3v$ (4)

and $J_e(a)$ is a Bessel function of order $\ell$ and argument

$$a = \frac{e\vec{k} \cdot \vec{E}_o}{m_e \omega_o^2} \quad . \tag{5}$$

Strictly speaking, this result only holds for an infinite uniform plasma: however we shall see shortly that for the parameters of interest here this dispersion relation is only very weakly dependent on the magnitudes of $\omega_{pe}$ and $\omega_{pi}$ (the electron and ion plasma frequencies) and consequently (3) may be expected to hold even for a strongly non-uniform plasma, provided that k and a are interpreted in some average sense.

Inserting the electron and ion distribution functions discussed above, and using the identity $\sum_{\ell=-\infty}^{\infty} J_\ell^2 = 1$, the dispersion relation may be written as

$$\left\{ \frac{\omega_{pi}^2}{k^2 v_i^2} \left[ \beta\, Z'\left( \frac{\omega - k v_1}{k v_{i1}} \right) + (1-\beta)\, Z'\left( \frac{\omega - k v_2}{k v_{i2}} \right) \right] \right\}^{-1}$$

$$= \sum_{\ell=-\infty}^{\infty} J_\ell^2(a) \frac{1}{1 - \frac{\omega_{pe}^2}{k^2 v_e^2} Z'\left( \frac{\omega + \ell\, \omega_o}{k v_e} \right)} \tag{6}$$

where $Z'(z)$ is the derivative of the Fried-Conté plasma dispersion function.

In the limit of zero applied electromagnetic field, this trivially reduces to

$$1 - \frac{\omega_{pe}^2}{k^2 v_e^2} Z'\left( \frac{\omega}{k v_e} \right) - \frac{\omega_{pi}^2}{k^2 v_i^2} \left[ \beta\, Z'\left( \frac{\omega - k v_1}{k v_{i1}} \right) + (1-\beta) Z'\left( \frac{\omega - k v_2}{k v_{i2}} \right) \right] = 0 \quad . \tag{7}$$

It is first necessary to interpret the oscillations having frequency $\frac{\omega_{1o}}{2\pi} = (515 \simeq 521)$kHz, $\frac{\omega_{2o}}{2\pi} = (542 \simeq 545)$kHz (data of second run for example). These acoustic oscillations are observed to occur spontaneously even in the limit $E_o = 0$. We find that they can be consistently interpreted as due to a streaming instability described by (7). This sets some fairly stringent (but physically acceptable) limits on the ion thermal velocities $v_{i1}$ and $v_{i2}$. If these thermal velocities exceed about 3500 m/sec, the streaming instability is suppressed by ion Landau damping; on the other hand they certainly exceed 1100 m/sec (which corresponds to a temperature of 300° K). Within this range, the precise value has a rather weak effect on the real part of $\omega$, and equation (7) possesses two unstable roots, having real parts slightly below $k\,v_1$ and $k\,v_2$ respectively. In fact, given these as first estimates, it is possible to reduce (7) to algebraic form by expanding the Fried-Conté functions for

$$\frac{\omega - k\,v_1}{k\,v_{i1}} \gg 1\ , \quad \frac{\omega - k\,v_2}{k\,v_{i2}} \gg 1\ , \quad \frac{\omega}{k\,v_e} \ll 1\ , \text{ and taking } \frac{\omega_{pe}}{k\,v_e} \gg 1:$$

$$\omega_{pi}^2 \left[ \frac{\beta}{(\omega - k\,v_1)^2} + \frac{(1-\beta)}{(\omega - k\,v_2)^2} \right] = \frac{2\,\omega_{pe}^2}{k^2 v_e^2} \left( 1 + i\,\frac{\sqrt{\pi}\,\omega}{k\,v_e} \right) \qquad (8)$$

and this equation gives a good approximation to the two unstable and the two most weakly damped roots of (7).

The upper unstable mode (i.e. that with greater real part of $\omega$) is significantly more unstable, and we have confirmed by computation with equation (6) that it remains so for all the parameters of this experiment, and this is consistent with the observation that the saturation amplitude

of this mode is always greater; indeed in some circumstances it is the only mode observed. Equation (8) shows that the modes which it describes are independent of the density of the plasma and have a phase velocity $\omega/k$ which is independent of k. These two properties in fact approximately hold for the corresponding roots of (6), although this is not readily demonstrated analytically, and this substantially simplifies the interpretation of the experiment.

Since Re $\omega_{1,2} \simeq k \cdot v_{1,2}$ one can at once infer an approximate value for k, which corresponds to a wavelength of about 20 cm, in reasonable agreement with the e-folding length for axial decay of the plasma density. We assume that this value of k corresponds to the eigenvalue of the normal mode which would be obtained if the plasma non-uniformity were treated in a fully consistent manner: in view of the independence of (8) of the density (until $\omega_{pe}$ has fallen to a value of order $k v_e$), this normal mode is thought to be fairly close to sinusoidal form, with a fixed wavelength determined by the density profile, so there is no serious inconsistency in using uniform plasma theory. The precise value of k, which does not vary with $E_o$ and $\omega_o$, cannot be calculated until the other parameters (such as $\beta$) have been determined, by using the observed variation of $\omega$ with $E_o$ and $\omega_o$. In view of this interpretation it is not surprising that slightly different k values are required to fit the upper and lower unstable modes.

To interpret the observed variation of $\omega$ with $E_o$ it is necessary to relate the field $E_o$, within the plasma to the RF voltage $V_{RF}$ applied between the

transmitter electrode and the whole of the metal vessel. Since the RF current exhibits between the RF electrodes the normal resonance probe characteristics (Fig. 5), we have assumed that conventional RF probe theory is applicable (e.g. Lekefi (1966)), so that the RF field in the plasma between the electrodes is:

$$E_o = \left( \frac{V_{RF}}{L} \right) \Big/ \left| 1 - \frac{S}{L} \frac{\omega_{pe}^2}{\omega_o (\omega_o - i \nu_{en})} \right| \qquad (9)$$

where S/2 is the ion sheath thickness on each RF electrode, L = 0.12 m is their separation, $\omega_{pe}$ the plasma frequency between the RF electrodes and $\frac{\nu_{en}}{2\pi}$ the dominant (electron-neutral) collision frequency which we estimated to be 1.25 MHz. From the peak of the resonant probe current characteristic one obtains the resonant frequency $\frac{\omega_R}{2\pi} = \left(\frac{S}{L}\right)^{\frac{1}{2}} \frac{\omega_{pe}}{2\pi}$ = 5 MHz (Fig. 5) and from the minimum one obtains the value of the plasma frequency between the RF electrodes; such a value agrees very well with the one deduced from the measured electron density profile $\frac{\omega_{pe}}{2\pi}$ = 11.3 MHz (Fig. 2). The ratio S/L is therefore known and equation (9) then gives $E_o$ for given $V_{RF}$ and $\omega_o$. This is then inserted into (5) taking the angle between $\vec{k}$ and $\vec{E}_o$ to be $\pi/4$ corresponding to the angle between the RF probe axis and the streaming direction.

The relation between the calculated value of the RF field $E_o$ (zero to peak), in the streaming direction and the applied RF voltage (r.m.s. value) is, for $\frac{\omega_o}{2\pi}$ = 5 MHz, following equation (9) = $E_o = V_{RF} \times 34.35$ where $E_o$ is in volts $m^{-1}$ and $V_{RF}$ is in volts. The dependence of $\omega_2$ (the

upper mode) upon $V_{RF}$, calculated in the above described manner, is in good qualitative agreement with the experimentally observed curve of the upper acoustic frequency shift (Figs. 9 and 10), for any reasonable choice of the remaining free parameters $\beta$, $v_{i1}$, $v_{i2}$, $v_e$. In every case $\omega_2$ increases with $V_{RF}$ up to a maximum around 5.5 volts (rms) and then decreases. The qualitative reasons for this can be seen if equation (6) is simplified by making the same approximations as were used to derive (8): in addition it is necessary to assume $\left(\frac{\omega_{pe}}{\omega_o}\right)^2 \gg 1$ and $\left(\frac{\ell\,\omega_o}{k\,v_e}\right)^2 \gg 1$ for all terms in the series except those with $\ell = 0, \pm 1$ (for $\ell = 1$, this is a bad approximation). One then obtains:

$$1 = \omega_{pi}^2 \left[\frac{\beta}{(\omega - k\,v_1)^2} + \frac{(1-\beta)}{(\omega - k\,v_2)^2}\right] \times \left[\frac{J_o^2}{\frac{2\,\omega_{pe}^2}{k^2 v_e^2}\left(1 + i\,\frac{\sqrt{\pi}\,\omega}{k\,v_e}\right)} + \right.$$

$$\left. + \frac{\omega_o^2}{\omega_{pe}^2}\left\{2\,J_1^2\left(1 - \frac{k^2 v_e^2}{\omega_o^2}\,\mathrm{Re}\left(\frac{1}{Z'\left(\frac{\omega_o}{k\,v_e}\right)}\right)\right) - \sum_{\ell} \ell^2\,J_\ell^2\right\}\right]. \quad (10)$$

This equation, like (8), represents the computed solutions of (6) for $\omega$ with an error of only $\sim$ 1%. For $E_o = 0$ the terms involving Bessel functions of order $\geq 1$ vanish and one recovers (8): as $E_o$ increases both the real and the imaginary parts of the second square bracket decrease, and the upper root consequently moves from a value somewhat below $k\,v_2$ up to a value close to $k\,v_2$. In fact the real part of $\omega_2$ reaches its maximum value slightly below $k\,v_2$, shortly after the real part of the second square bracket passes through zero, and before the imaginary part reaches zero; likewise the lower mode starts from a value somewhat below

$k\ v_1$, and rises towards $k\ v_1$. In fact the real part of $\omega_1$ passes slightly above $k\ v_1$ and there saturates, and the imaginary part of $\omega_1$ becomes large as the real part passes through $k\ v_1$. For very small values of $E_o$, the lower mode was not always found to be unstable: as $v_{i_1}$ is increased, ion Landau damping tends to stabilize it before the upper mode. The behaviour described above is in good qualitative agreement with the experimental observations. Because the upper mode has the higher growth rate for all values of $E_o$, it is more readily distinguished from the turbulent spectrum which the instability generates, and in consequence we have used its dependence on $E_o$ for fixed $\frac{\omega_o}{2\pi}$ = 5 MHz to determine the value of the free parameters. The agreement between the theoretical fractional frequency shift $[\omega_2(E_o) - \omega_2(o)]/\ \omega_2(o)$ and the experimental values, for the optimum choice of these parameters, is shown in Fig. 9, for the case of the first experimental run and in Fig. 10 for the case of the second run.

Using these same distribution function parameters, we then calculated the frequency shift for the lower mode. The comparison of the theoretical curve with the experimental values of the lower mode, is shown in Fig. 11 (data of the second run). The data presented in Figs. 7 and 8 (first run) are compared with the theory by first calculating from equation (9) the values of $E_o$, for constant applied radio-frequency voltage $V_{RF}$ = 5.5 volt (rms), but for varying values of $\omega_o$. The fractional frequency shifts, as a function of

$\omega_o/2\pi$, for the upper and for the lower modes, are then calculated for these values of $E_o$, using the values of the distribution function parameters $v_e$, $v_{i1}$, $v_{i2}$, $\beta$ already estimated for the first experimental run. The RF electric field $E_o$ is maximum at the sheath-plasma resonance and this behaviour is reflected in the maximum presented by the frequency shifts of the upper and lower modes, for the resonance condition at $\frac{\omega_o}{2\pi} = 5$ MHz.

The absolute values of k used to derive the left-hand scales in Figs. 7 - 11 were obtained experimentally from the value of $\omega$ at $V_{RF} = 0$. The values are, as we have seen, in good qualitative agreement with that which would be expected from the plasma density profile, and we have given grounds for expecting that k would not vary significantly with $V_{RF}$. It is less certain that the distribution functions remained the same throughout the whole of each run and such variations may have occurred between the recording of the data used to construct figs. 7 and 9 respectively (for example). The assumption that such variations did not occur may well account for the less precise agreement between the theoretical frequency shifts and the experimental values, in the measurement where $\omega_o$ is varied for constant $V_{RF}$.

During the RF injection, up to $V_{RF} = 10$ volt (rms), the electron temperature was monitored to be constant. The effect of the experimental uncertainty in the measurement of $T_e$, by the Langmuir probe method, on the calculated values of the acoustic frequency, was estimated

numerically. An experimental uncertainty in the value of $T_e$ of 10% produces a variation in $\frac{\omega}{2\pi}$ of 1 kHz, which is negligible compared with the RF induced shift.

## 5. DISCUSSION

The parametric instability has been the subject of extensive study. Stern, R.A. and Tzoar, N. (1966) observed the excitation of electron plasma and ion acoustic waves by means of an electromagnetic wave at $\omega \sim \omega_{pe}$ ; such an effect was analysed theoretically by Du Bois, D.F. and Goldman, M.V. (1967), by Goldman, R. (1969) and by Nishikawa, K. (1968). Parametric excitation of drift waves was observed (Wong, A.Y., Goldman, M.V., Hai, F. and Rowberg, R. (1968)). More recently the decay instability of longitudinal electron plasma waves was reported (Franklin, R.N., Hamberger, S.M., Lampis, G. and Smith, G.J. (1971)) as well as the study of its saturation (Stenzel, R. and Wong, A.Y. (1972)). The anomalous heating of a one dimensional plasma by parametrically excited ion fluctuations has been described in a computer experiment by Kruer, W.L., Kaw, P.K., Dawson, J.M. and Oberman, C. (1970).

The frequency shift of drift waves, in the presence of a high frequency field, was observed and was qualitatively explained as due to the increase of the electron temperature, which is proportional to the drift wave frequency (Demirkhanov, R.A., Khorasanov, G.L. and Sidorova, I.K. (1971)). The frequency shift of ion acoustic waves, due to the presence of a high frequency field, has been studied theoretically, for the case of a plasma with Maxwellian ions

and electrons, by Kaw, P.K. and Dawson, J.M. (1970) following the analysis of Sanmartin, J.R. (1970) of the Vlasov equation. More recently Porkolab, M. (1972), using the dispersion equation of Silin, obtained growth rates and thresholds for the parametric instability of short wavelength ion acoustic waves and calculated the shift of their frequency, due to the presence of an external high frequency electric field, for the case of a plasma having Maxwellian ions and electrons.

In the case of our experiment, where the electrons are thermal, but where the ions consist of a double energy beam, the dispersion equation (4.8) of Silin, V.P. (1965) had to be evaluated "ad hoc". The theory of Silin explains well the observed frequency shifts of the double acoustic wave present in our plasma, when it is coupled parametrically to the RF pump; the saturation of the shift is also explained.

We have, however, only verified that part of the theory which refers to the linear phase of the instability and not the part related to the build-up of the turbulent spectrum (Silin, V.P. (1969)). However our observations bear upon the non-linear outcome of the instability, because for values of $V_{RF} < 10$ volt (rms), we have not had to take into account the variation of the plasma parameters with the RF field, in order to explain the frequency observations. At the value of $V_{RF} = 10$ volt (rms), at which the experiment was cut off, corresponding to an electric field in the streaming direction $E_o = 343$ volt $m^{-1}$ (zero to peak), the growth rate of the parametric resonance instability has grown to the value of 10% of the real part of the frequency, and experimentally

this correlated with the flattening out of the acoustic spectrum for the $V_{RF}$ > 10 volt (rms) (Fig. 6f). This flattening of the spectrum is due in part to the increase of the growth rate of the lower mode and the decrease in the growth rate of the upper mode, as the electron temperature increases, but doubtless other non-linear processes are involved.

ACKNOWLEDGMENTS

It is a pleasure to acknowledge many interesting discussions with Professor K. Takayama, Drs S.Hamberger, H. Ikezi, A. Samain, M. Cotsaftis and D. Lepechinski.

REFERENCES


1. AIHARA, S, LAMPIS, G. and TAKAYAMA, K. (1968) Phys. Lett. 28A, 5, 352.
2. AIHARA, S., TAKAMURA, S. (1971) Appl. Phys. Lett. 18, 375.
3. AIHARA, S. TAKAMURA, S., LAMPIS, G. (1970), Kakuyugokenkyu 25, 2, 92.
4. ALIEV YU. M. and SILIN, V.P. (1965) ZhETF, 48, 901. [(1965) Sov. Phys. JETP 21, 601].
5. ALIEV YU. M., SILIN, V.P., WATSON, C.J.H. (1966) ZhETF, 50, 943. [(1966) Sov. Phys. JETP 23, 626].
6. ANDREEV, N.E., KIRYI A. YU. and SILIN, V.P. (1969) ZhETF 57, 1024 [(1970) Sov. Phys, JETP, 30, 559].
7. BATANOV, G.M., SARKSIAN, K.A., SILIN, V.P. (1969) Proc. Bucharest Conf. Phenomena in Ionised Gases, p.541.
8. BEKEFI, G. (1966), Radiation processes in Plasmas, J. Wiley, p.168.
9. DEMIRKHANOV, R.A., KHORASANOV, G.L., SIDOROVA, I.K. (1970) ZhETF 59, 1873. [(1971) Sov. Phys. JETP, 32, 1013].
10. DU BOIS, D.F. and GOLDMAN, M.V. (1967), Phys. Rev. 164, 207.
11. FAINBERG, YA. B. and SHAPIRO, V.D. (1967) ZhETF, 52, 293 [(1967) Sov. Phys. JETP 25, 189].
12. FRANKLIN, R.N., HAMBERGER, S.M., LAMPIS, G. and SMITH, G.J. (1971) Phys. Rev. Lett. 27, 1119.
13. GEKKER, I.R., SIZUKHIN, O.V. (1969) Proc. Bucharest Conf. Phenonena in Ionised Gases, p.502.
14. GOLDMAN, R. (1969) Phys. Fluids 12, 662,
15. GORBUNOV, L.M. (1969) ZhETF 56, 1693. [(1969) Sov. Phys. JETP 29, 907].

16. HARP, R.S. and CRAWFORD, F.W. (1964) J. Appl. Phys. 35, 3436.

17. KAW, P.K. and DAWSON, J.M. (1969) Phys. Fluids 12, 2586.

18. KAW, P.K. and DAWSON, J.M. (1970) Princeton Plasma Physics Laboratory Rep. MATT 802.

19. KAWAI, Y. LAMPIS, G. AIHARA, S. and KAWABE, T. (1969) J, Phys. Soc. Jap. 26, 578.

20. KORNILOV, E.A. FAINBERG Ya. B., BOLOTIN, L.I. and KOVPIK, O.F. (1966) ZhETF, Pis'ma 3, 9, 354. [(1966) JETP Lett. 3, 229].

21. KRIVORUCHKO, S.M., KORNILOV, E.A. (1969) ZhETF, Pis.Red. 10, 10, 465. [(1969) JETP Lett. 10, 10, 299].

22. KRUER, W.L., KAW, P.K., DAWSON, J.M. and OBERMAN, C. (1970) Phys. Rev. Lett. 24, 987.

23. LAMPIS, G. AIHARA, S. and TAKAYAMA, K. (1968) Phys. Lett. 28A, 197.

24. MOTZ, H. and WATSON, C.J.H., Adv. in Electronics and Electron Physics 23, 153.

25. NISHIKAWA, K. (1968), J. Phys. Soc. Jap. 24, 916.

26. PORKOLAB, M. (1972) Nucl. Fusion 12, 329.

27. SANMARTIN, J.R. (1970) Phys. Fluids 13, 1533.

28. SERGHEICHEV, K.F. (1969) Proc. Bucharest Conf.Phenomena in Ionised Gases, p.540.

29. SILIN, V.P. (1965) ZhETF 48, 1679. [(1965) JETP 21, 1127].

30. SILIN, V.P. (1966) ZhETF 51, 1842 [(1967) JETP 24, 1242].

31. SILIN, V.P. (1969) ZhETF 57, 183. [(1970) JETP 30, 105].

32. STENZEL, R. and WONG, A.Y. (1972) Phys. Rev. Lett. 28, 274.

33. STERN, R.A. and TZOAR, N. (1966) Phys. Rev. Lett. 17, 903.

34. TAKAMURA, S. AIHARA, S. and TAKAYAMA, K. (1970), Phys. Fluids 13, 3052.

35. TAKAMURA, S. AIHARA, S. and TAKAYAMA, K. (1971) J.Phys. Soc.Jap. 31, 3, 925.

36. TAKAMURA, S. TANAKA, Y. and OKUDA, T. (1969) Kakuyugokenkyu 23, 192.

37. TAKAYAMA, K. IKEGAMI, H. AIHARA, S. (1967) Proc. Eighth Int. Conf. Phenomena Ionised Gases, Vienna, paper 6, 3, 3.

38. TAKAYAMA, K., IKEGAMI, H. and MIYAZAKI, S. (1960) Phys. Rev. Lett. 5, 238.

39. WONG, A.Y., GOLDMAN, M.V., HAI, F. and ROWBERG, R. (1968) Phys. Rev. Lett. 21, 518.

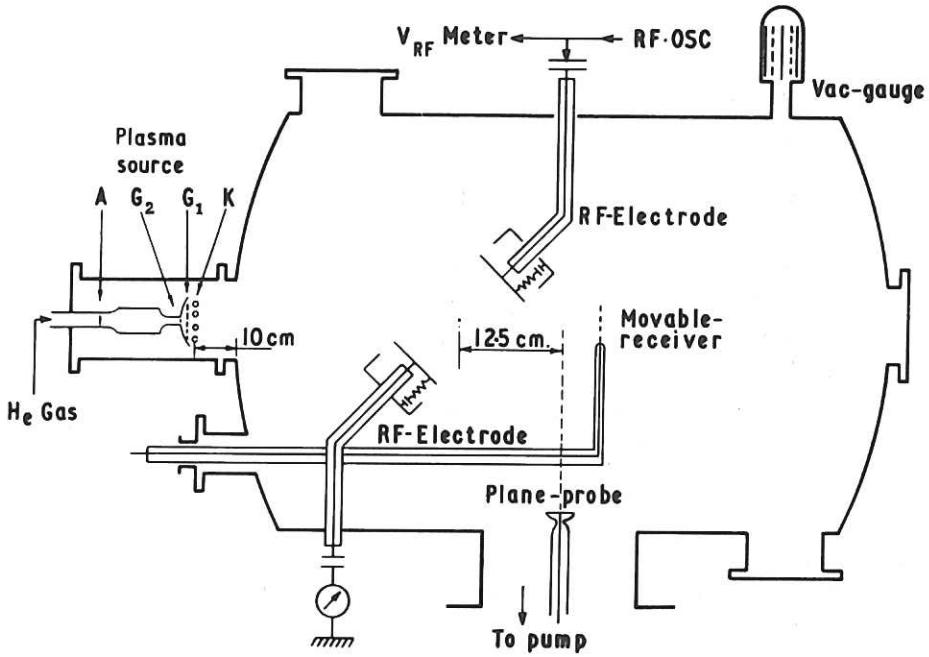


Fig.1 Experimental apparatus. A = anode; $G_1$, $G_2$ : acceleration grids; K = cathodes.

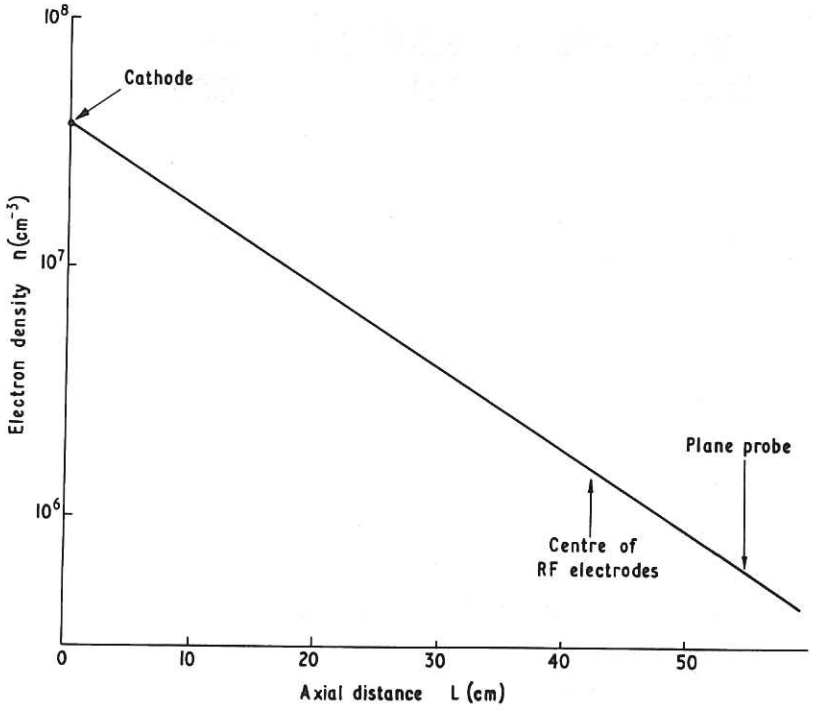


Fig.2 Axial electron density profile during the two interpreted radiofrequency injection runs. CLM-P 335

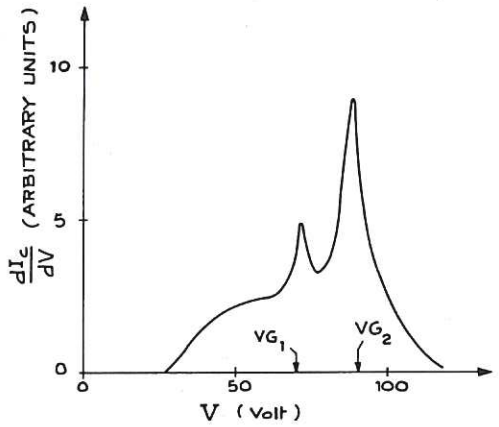


Fig.3 Typical ion energy distribution, measured 6 cm away from the cathodes. ($VG_1$ = + 70 volt; $VG_2$ = + 90 volt). $I_c$ is the ion collected current; V is the ion energy in volts.

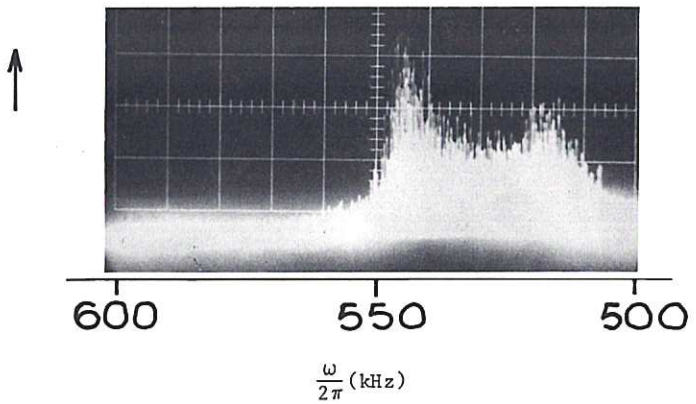


Fig.4 Frequency spectrum of the fundamental ion acoustic waves. No RF field injected. (Second experimental run.) Horizontal scale = 10 kHz/div. Vertical scale = Amplitude linear (arbitrary units).

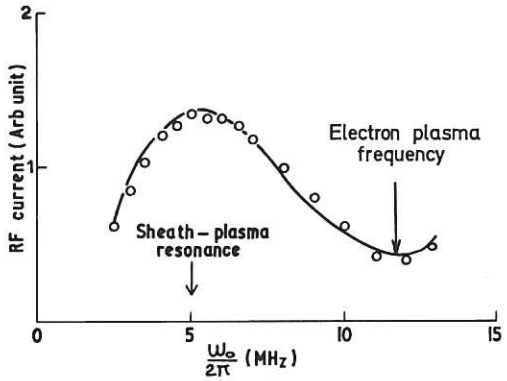


Fig.5 Resonance probe characteristic during the two interpreted radio-frequency injection runs. Distance between RF electrodes = 12 cm. CLM-P 335

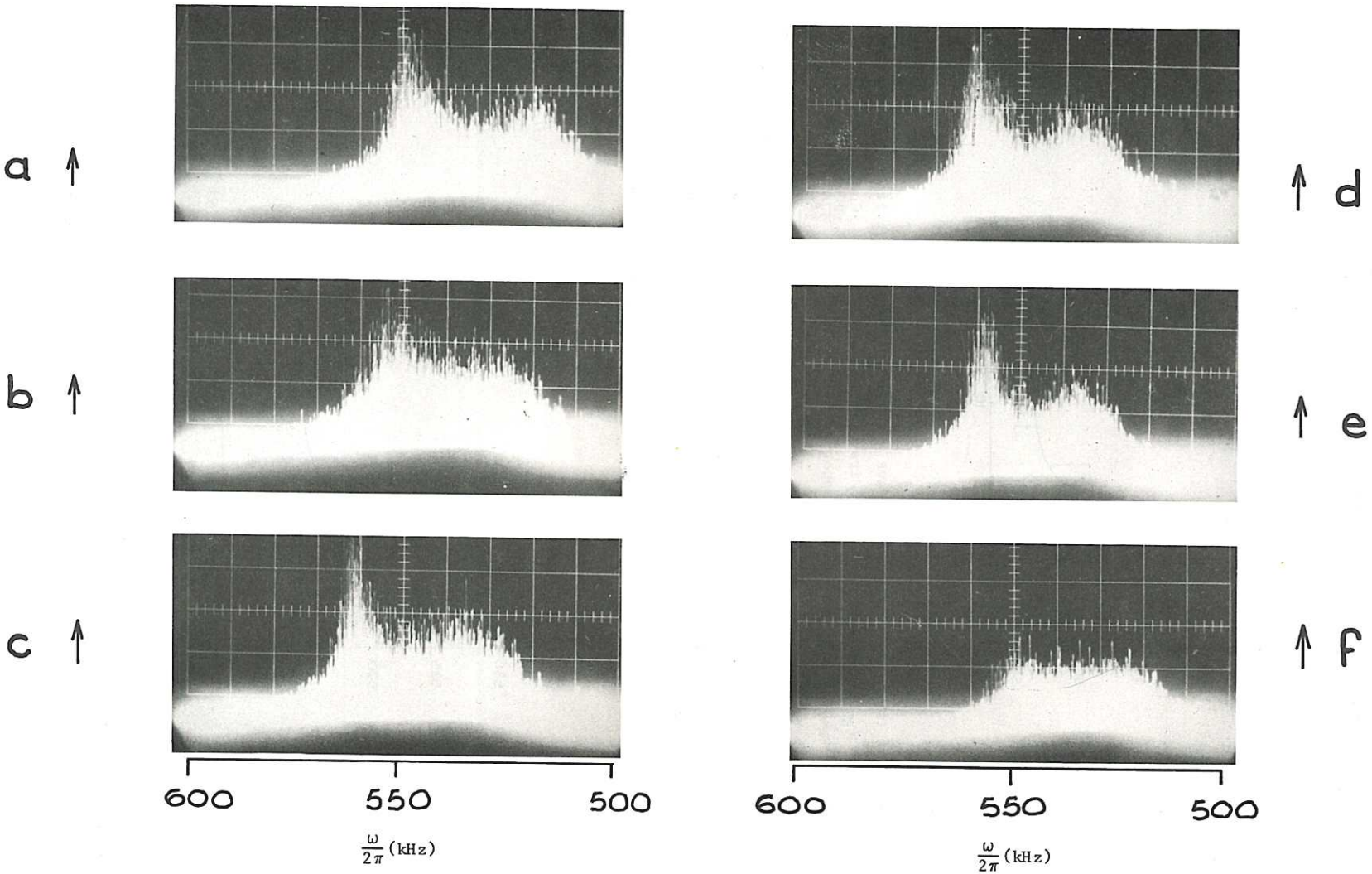


Fig.6 Frequency spectrum of the fundamental ion acoustic waves during the radiofrequency injection (second experimental run) for constant value of $\frac{\omega_0}{2\pi}$ (5 MHz) and for variable $V_{RF}$ (volt rms). (a): $V_{RF}$ = 2V; (b) $V_{RF}$ = 3V; (c) $V_{RF}$ = 5V; (d) $V_{RF}$ = 7V; (e) $V_{RF}$ = 9V; (f) $V_{RF}$ = 15V. Horizontal scale = 10 kHz/div. Vertical scale = Amplitude linear (arbitrary units).

CLM-P 335

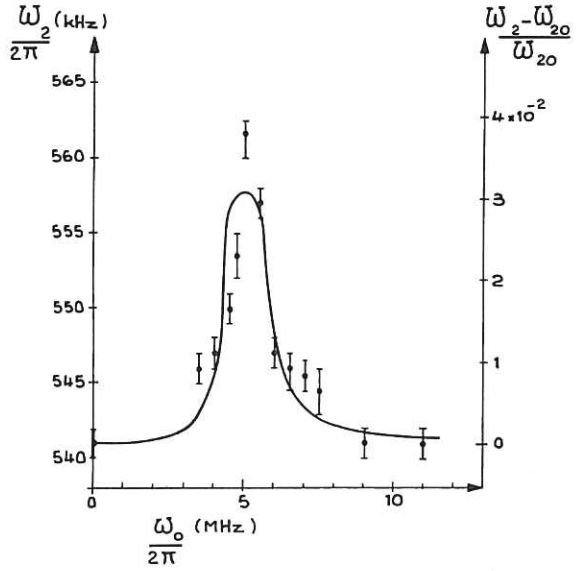


Fig.7 Frequency of the upper ion acoustic wave $\frac{\omega_2}{2\pi}$, versus frequency $\frac{\omega_o}{2\pi}$ of the RF electric field for constant $V_{RF}$ = 5.5 volt (rms). (First experimental run). Continuous line = theory. $\frac{\omega_{20}}{2\pi}$ = 541 kHz : initial value of upper acoustic frequency. $\frac{k_2}{2\pi}$ = 4.62 $m^{-1}$. Parameters: $v_e = 6 \times 10^5$ m/sec; $\beta$ = 0.162; $v_{i2}$ = 1400 m/sec; $R = \frac{v_{i2}}{v_{i1}}$ = 0.801.

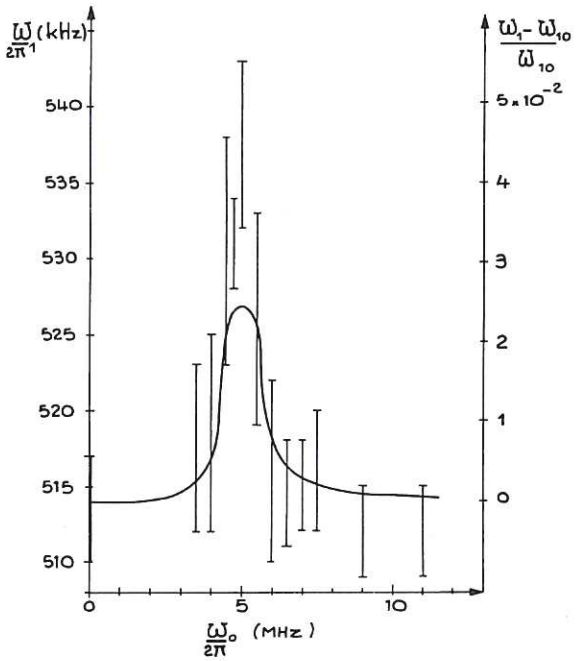


Fig.8 Frequency of the lower ion acoustic wave $\frac{\omega_1}{2\pi}$ versus frequency $\frac{\omega_o}{2\pi}$ of the RF electric field, for constant $V_{RF}$ = 5.5 volt (rms). (First experimental run). Continuous line - theory. $\frac{\omega_{10}}{2\pi}$ = 514 kHz : initial value of lower acoustic frequency. $\frac{k_1}{2\pi}$ = 4.66 $m^{-1}$. Parameters: $v_e = 6 \times 10^5$ m/sec; $\beta$ = 0.162; $v_{i2}$ = 1400 m/sec; $R = \frac{v_{i2}}{v_{i1}}$ = 0.801.

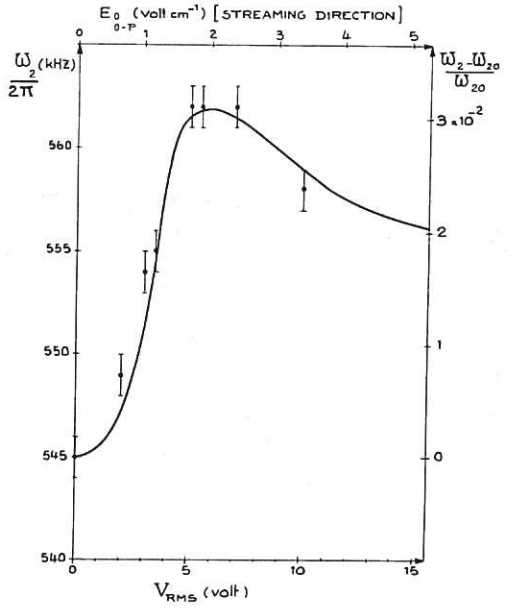


Fig.9 Frequency of the upper ion acoustic wave $\frac{\omega_2}{2\pi}$ versus applied RF voltage, for constant $\frac{\omega_o}{2\pi}$ = 5 MHz (sheath-plasma resonance). (First experimental run). Continuous line = theory. $\frac{\omega_{2o}}{2\pi}$ = 545 kHz : initial value of upper acoustic frequency. $\frac{k_2}{2\pi}$ = 4.66 $m^{-1}$. Parameters: $v_e = 6 \times 10^5$ m/sec; $\beta$ = 0.162; $v_{i2}$ = 1400 m/sec; $R = \frac{\omega_{i2}}{v_{i1}}$ = 0.801.

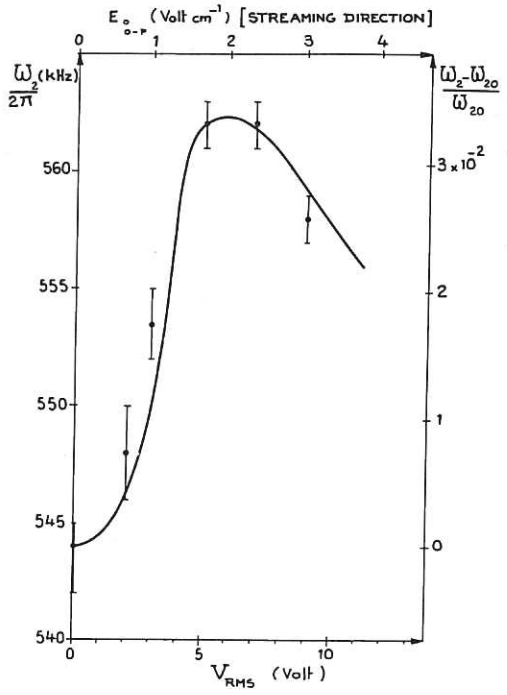


Fig.10 Frequency of the upper ion acoustic wave $\frac{\omega_2}{2\pi}$ versus applied RF voltage, for constant $\frac{\omega_o}{2\pi}$ = 5 MHz (sheath-plasma resonance). (Second experimental run). Continuous line = theory. $\frac{\omega_{2o}}{2\pi}$ = 544 kHz : initial value of upper acoustic frequency. $\frac{k_2}{2\pi}$ = 4.78 $m^{-1}$. Parameters: $v_e = 6 \times 10^5$ m/sec; $\beta$ = 0.228; $v_{i2}$ = 1800 m/sec; $R = \frac{v_{i2}}{v_{i1}}$ = 0.832.

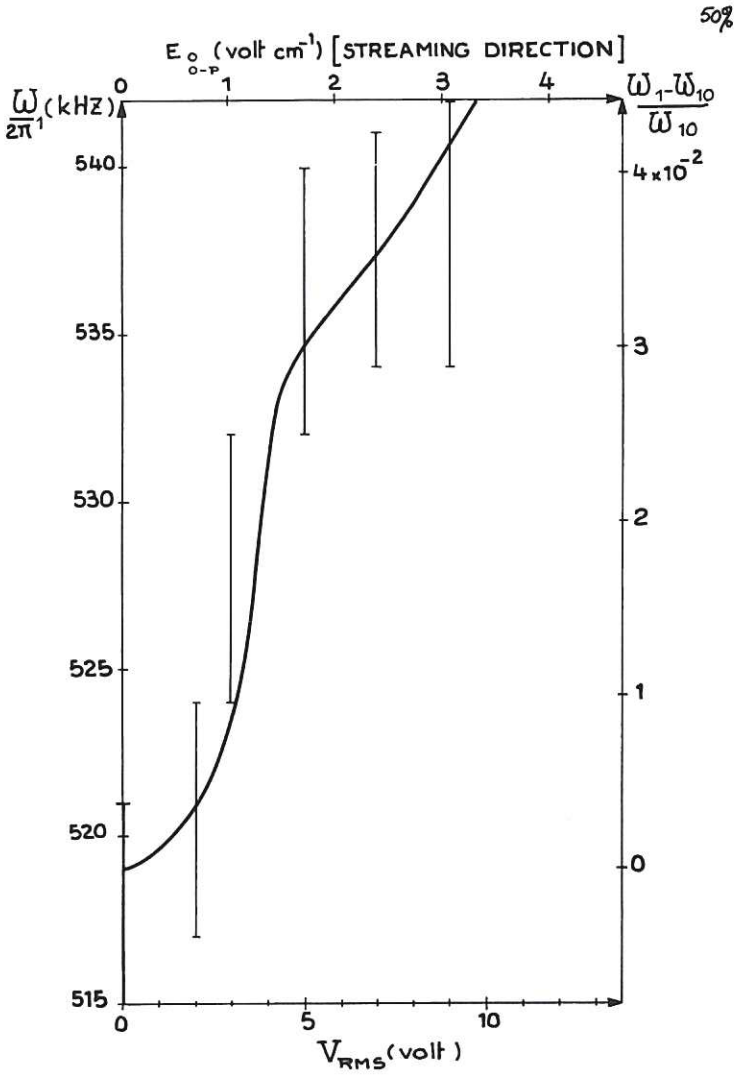


Fig.11 Frequency of the lower ion acoustic wave $\frac{\omega_1}{2\pi}$ versus applied RF voltage, for constant $\frac{\omega_o}{2\pi}$ = 5 MHz (sheath plasma resonance). (Second experimental run). Continuous line = theory. $\frac{\omega_{1o}}{2\pi}$ = 519 kHz : initial value of lower acoustic frequency. $\frac{k_1}{2\pi}$ = 4.91 $m^{-1}$. Parameters: $v_e = 6 \times 10^5$ m/sec; $\beta = 0.228$; $v_{i2} = 1800$ m/sec; $R = \frac{v_{i2}}{v_{i1}} = 0.832$. CLM-P 335